Control of the light transmission through a quasiperiodic waveguide

Priya Rose T., Gianluigi Zito, Emiliano Di Gennaro,* Giancarlo Abbate, and Antonello Andreone

CNR-SPIN and Department of Physical Sciences, Universitá di Napoli "Federico II," Naples, Italy

**emiliano.digennaro@na.infn.it*

Abstract: We studied the waveguiding properties of a photonic quasicrystal based on an octagonal tiling. The structure exhibits intrinsic localisation in the band gap region, that can be exploited to manipulate the signal transmission through a linear defect. The electromagnetic characteristics are first numerically analysed using a full wave simulation and then experimentally verified by measurements carried out in the X-band microwave region. Possible photonic applications include tunable notch filters having large attenuation.

OCIS codes: (050.5298) Photonic crystals; (130.5296) Photonic crystal waveguides.

References and links

1. A. Della Villa, S. Enoch, G. Tayeb, V. Pierro, V. Galdi, and F. Capolino, "Localized modes in photonic quasicrystals with Penrose-type lattice," Phys. Rev. Lett. **94**, 183903 (2005).
2. Y. Wang, Y. Wang, S. Feng, and Z.-Y. Li, "The effect of short-range and long-range orientational orders on the transmission properties of quasiperiodic photonic crystals," Europhys. Lett. **74**, 49–54 (2006).
3. C. Jin, B. Cheng, B. Man, Z. Li, D. Zhang, S. Ban, and B. Sun, "Band gap and wave guiding effect in a quasiperiodic photonic crystal," Appl. Phys. Lett. **75**, 1848–1850 (1999).
4. M. Zoorob, P. G. Charlton, M. D. B., J. Baumberg, and M. Netti, "Complete and absolute photonic bandgaps in highly symmetric photonic quasicrystals embedded in low refractive index materials," Mat. Scien. and Eng. B **74**, 168–174 (2000).
5. M. Florescu, S. Torquato, and P. J. Steinhardt, "Complete band gaps in two-dimensional photonic quasicrystals," Phys. Rev. B **80**, 155112 (2009).
6. T. PriyaRose, E. Di Gennaro, G. Abbate, and A. Andreone, "Isotropic properties of the photonic band gap in quasicrystals with low-index contrast," Phys. Rev. B **84**, 125111 (2011).
7. A. Della Villa, S. Enoch, G. Tayeb, V. Pierro, V. Galdi, and F. Capolino, "Localized modes in photonic quasicrystals with penrose-type lattice," Opt. Express **14**, 10021–10027 (2006).
8. Y. Neve-Oz, T. Pollok, S. Burger, M. Golosovsky, and D. Davidov, "Resonant transmission of electromagnetic waves through two-dimensional photonic quasicrystals," J. Appl. Phys. **107**, 063105 (2010).
9. Y. Wang, X. Hu, X. Xu, B. Cheng, and D. Zhang, "Localized modes in defect-free dodecagonal quasiperiodic photonic crystals," Phys. Rev. B. **68**, 165106 (2003).
10. G. Zito, T. Priya Rose, E. Di Gennaro, A. Andreone, E. Santamato, and G. Abbate, "Bandgap properties of low-index contrast aperiodically ordered photonic quasicrystals," Microw. Opt. Technol. Lett. **51**, 2732–2737 (2009).
11. Simulation software package developed at MIT, (http://ab-initio.mit.edu/wiki/index.php/Meep).
12. Harminv, (cfr. http://ab-initio.mit.edu/wiki/index.php/Harminv).
13. See for example the 6th chapter of "*Photonic Crystals: Molding the Flow of Light*," John D. Joannopoulos, Robert D. Meade, and Joshua N. Winnfree (Princeton University Press, 2008)
14. S. Savo, E. Di Gennaro, and A. Andreone, "Superlensing properties of one-dimensional dielectric photonic crystals," Opt. Express **17**, 19848–19856 (2009).
15. S. Fan, P. Villeneuve, J. Joannopoulos, and H. Haus, "Channel drop filters in photonic crystals," Opt. Express **3**, 4–11 (1998).

16. J. Romero-Vivas, D. Chigrin, A. Lavrinenko, and C. S. Torres, "Resonant add-drop filter based on a photonic quasicrystal," Opt. Express **13**, 826–835 (2005).

1. Introduction

Unlike their periodic counterparts, the electromagnetic (EM) properties of photonic quasicrystals (PQCs) are strongly dependent on the short-range order of the lattice [1,2]. Because of their structural peculiarities such as a higher order of rotational symmetries (> 6, not allowed for periodic crystals) and the presence of many non-equivalent sites, PQCs can present novel and interesting features, including highly isotropic and low index contrast band gaps [3–6] and intrinsic localisation both in transparency [7,8] and in stop bands [5,9]. In particular, contrarily to what happens in the periodic case, some aperiodically ordered photonic crystals show localised modes without intentionally created defects, affecting the EM response of devices based on these peculiar structures. In this letter, we use a full wave analysis to study the transmission of light in a linear waveguide based on a specific geometry with 8-fold rotational symmetry having intrinsic localisation in a photonic band gap (PBG) frequency region. We show that the waveguide response can be controlled introducing an additional defect in close proximity of the localised mode. These peculiar characteristics are then experimentally verified performing signal transmission and electric field spatial measurements in a quasicrystalline structure operating in the X-band microwave region.

Samples and method

The 2D quasiperiodic geometry is based on the interference pattern of 8 coherent beams according to the following formula for the irradiance profile:

$$I(\mathbf{r}) = \sum_{l=1}^{8} \sum_{m=1}^{8} A_l A_m^* \exp[i(\mathbf{k}_l - \mathbf{k}_m) \cdot \mathbf{r} + i(\phi_l - \phi_m)] \tag{1}$$

where A_l, k_l, and ϕ_l are the amplitudes, the wavevectors, and the initial phases of the interfering beams, respectively. The phase of the interfering beams is periodically shifted by $\frac{\pi}{2}$, such that $\phi_1 = \phi_5 = 0$, $\phi_2 = \phi_4 = \phi_6 = \phi_8 = \frac{\pi}{2}$, and $\phi_3 = \phi_7 = \pi$. The wave vectors $\mathbf{k}_l$ of the beams are equally distributed along the (x,y)-plane, whereas all the beams are linearly polarized along the z direction. The scatterers are represented by infinitely long dielectric rods (principal axis along the z direction) displaced to occupy the regions where the interference pattern shows its local maxima. Their position is determined by choosing a threshold value for the light intensity level. Fixing also the rods radius, the filling factor η, defined as the ratio between the regions showing a high refractive index and the total area, is determined [10].

The sample under study in this work is a finite square tiling composed of 365 cylindrical rods of alumina (dielectric constant $\varepsilon = 8.6$) with radius $r = 0.3a$, where a is a characteristic length, and filling factor $\eta = 0.26$. Crystal parameters have been optimised to ensure the formation of clear PBG regions, avoiding at the same time the overlapping of the scatterers. The rods are placed in air according to the 8-fold symmetrical pattern described by Eq. (1), as shown in Fig. 1.

To study EM propagation properties through the sample, numerical simulations are performed by using MEEP [11], a freeware code which uses the finite difference time domain (FDTD) method. Space discretization is set to have a grid resolution of $0.067a$, which ensures a number of pixels per wavelength in the range from 40 to 60. Perfectly matched layers, surrounding the whole area, are included to avoid spurious reflections from the boundaries. A time-pulsed collimated Gaussian beam with TM polarization (electric field parallel to the rod axis) and a waist of $10a$ is impinging on the sample from the left side (continuous line in Fig. 1).

#160960 - $15.00 USD Received 4 Jan 2012; revised 28 Feb 2012; accepted 5 Mar 2012; published 2 Nov 2012

Transmitted fluxes are recorded at the right side in a position specular to the source (dotted line in Fig. 1), normalized in respect to the vacuum case, and analyzed by using a field discrete Fourier transform.

2. Results

As a first step, we characterize the transmission properties of the full structure (FS) as a function of the normalized frequency a/λ, where λ is the signal wavelength, in the range $0.1-0.8$. In this region different PBG regions are present, however we focus our attention on the wider one, spanning from 0.26 to 0.34, since it includes a local higher transmittance region around the normalized frequency of 0.335 (Fig. 2, full line). The presence of this tiny peak suggests the occurrence of a light localization phenomenon, even in absence of an extrinsic defect of the quasiperiodic tiling.This is confirmed by the response of the PQC structure at that specific frequency to an almost monochromatic pulse. The computed field distribution inside the sample puts in evidence a fairly strong localization around the central post (in the x-y axes origin of Fig. 1), and the analysis of the field time evolution by means of a free-ware harmonic inversion tool [12] allows to estimate the resonance quality factor of this doubly degenerate mode be approximately 6000.

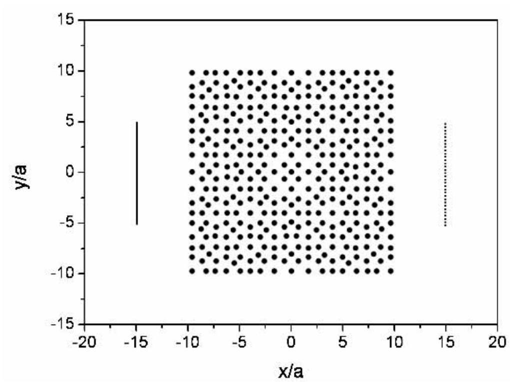

Fig. 1. 8-fold quasicrystalline finite structure. Continuous line represents the current source of the incoming collimated beam, whereas dashed line is the field intensity monitor.

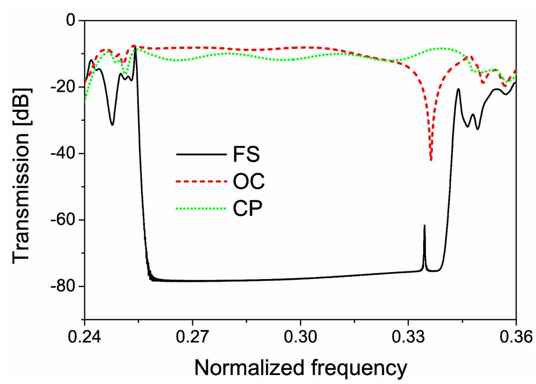

Fig. 2. Simulated transmission properties of the PQC full structure (FS, full line), with a linear defect (OC, dashed line), and with a linear defect and central pillar (CP, dotted line).

#160960 - $15.00 USD Received 4 Jan 2012; revised 28 Feb 2012; accepted 5 Mar 2012; published 2 Nov 2012

We then design a linear waveguide (OC) creating an open channel within the structure by removing all rods in a central strip having a lateral size of 2.75a. As expected, the OC frequency response shows a high transmission level in all the bandgap regions, but a marked dip in close proximity of the localized mode, specularly to the local maximum exhibited by the full structure in the main PBG (Fig. 2, dashed line). Indeed, the presence of a linear defect passing through the middle of the PQC sample does not produce a significant effect on the localization properties, slightly changing only the resonance frequency of the mode.

To better understand the influence of localisation in the waveguide properties, we show in Fig. 3(a) the electric field map produced by a continuous wave source at the localized mode frequency. The radiation travels throughout the waveguide until it reaches the position where the central pillar should be, behind this point the light propagation is inhibited. The analysis of the field map time evolution indicates the presence of standing waves inside the waveguide, which represents a clear evidence that the light is reflected back in correspondence of the channel midpoint, giving rise to the transmission dip shown in Fig. 2.

We then study the influence of a mode perturbation on the transmission properties of the PQC linear waveguide. We consider the sample with an open channel and an additional pillar placed in its center (CP) (x-y origin). As it can be seen from (Fig. 2 (dotted line), signal transmission is fully restored at the localized mode frequency and is almost unaffected in the remaining part of the frequency range analyzed. It is also clear from the electric field map shown in Fig. 3(b) that, when the central pillar is present, reflection is strongly damped and light can pass through the whole waveguide as it would happen in a simple periodic linear waveguide [13]. If 'milder' pertubations are considered, the localized mode can be tuned. Indeed, decreasing the dielectric constant or the radius of the pillar, a dip in the transmission characteristics appears and becomes more and more evident, whereas the frequency gradually downshifts until the overall e.m. response superimposes on what observed in the OC case. Similar effect can be also observed by gradually misplacing the pillar from the central position.

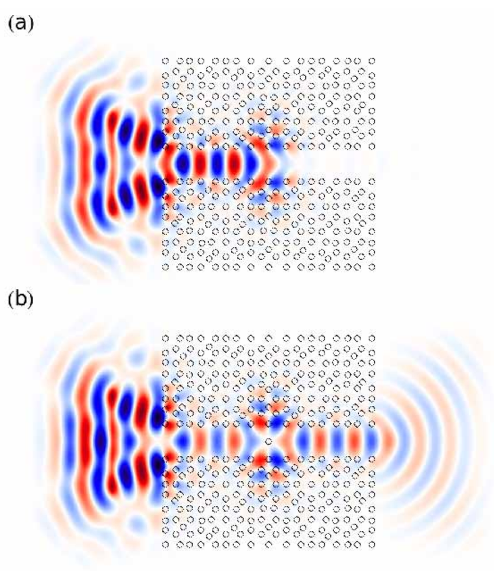

Fig. 3. Electric field z-component spatial maps for the OC sample (a) and the CP sample (b) at the normalised frequency 0.335 where the localised mode occurs.

In order to experimentally verify these results, we designed and carried out measurements

#160960 - $15.00 USD Received 4 Jan 2012; revised 28 Feb 2012; accepted 5 Mar 2012; published 2 Nov 2012

in the microwave region. The samples are realized by arranging alumina rods having height $h = 1cm$ and permittivity $\varepsilon = 8.6$ in a parallel plate waveguide [14]. The pillar radius is $r = 0.3cm$ and the characteristic length is $a = 1cm$, so that the EM bandgap of the structure is in the range $8 - 10GHz$. An $X - Y$ robot realized using a stepper motor is used both to place the rods according to the interferential pattern and to map the electric field in the different configurations (FS, OC, CP). The scattering parameters are measured using two monopole antennas connected to a vectorial network analyzer HP8720C. Microwave absorbing foams are used to prevent spurious reflections from the boundaries of the finite structure. A top view of the experimental setup is displayed in the inset of Fig. 3.

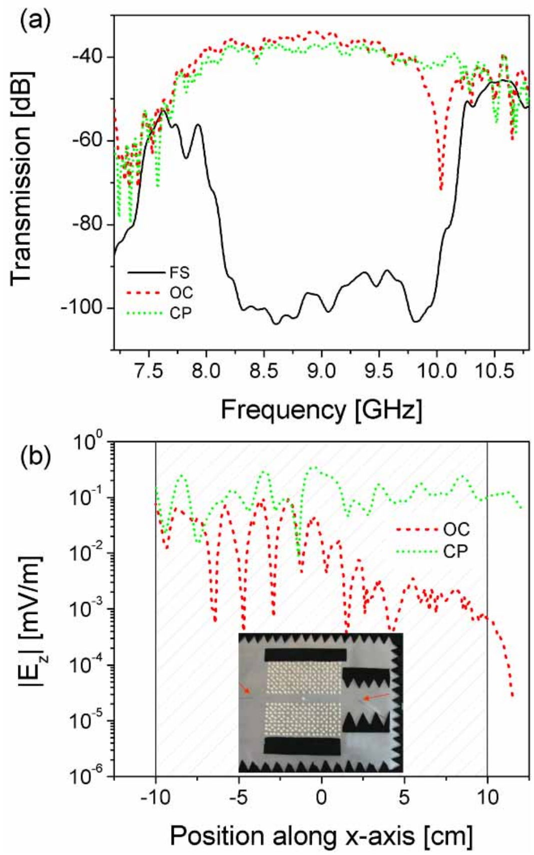

Fig. 4. (a): Transmission properties of the PQC full structure (FS), with a linear defect (OC), and with a linear defect and central pillar (CP). (b): Electric field intensity spatial profile along the linear waveguide for the OC sample and the CP sample at the localised mode frequency $10.06GHz$. The gray patterned area indicates the region along the x-axis occupied by the quasicristalline structure. In the inset a top view of the experimental setup. Red arrows indicate the position of the two monopole antennas.

Measured transmission characteristics around the PBG region (corresponding to the normalized frequency range 0.24-0.36) for the three configurations (FS, OC, and CP) are shown in Fig. 4(a), in good agreement with the simulation results. In the FS case the resonance peak is partially masked, likely due to the effect of losses introduced by the metallic plates and not included in the 2D simulations. The spatial field profile for the localised mode at $10.06GHz$ is shown in Fig. 4(b), highlighting the marked difference in the signal propagation with and

#160960 - $15.00 USD Received 4 Jan 2012; revised 28 Feb 2012; accepted 5 Mar 2012; published 2 Nov 2012

without the central dielectric pillar in the waveguide. The presence of the central pillar clearly modifies the light transmission at the frequency corresponding to the localized state. The signal is restored and travels through the linear waveguide almost unaffected.

3. Conclusion

We have numerically found and experimentally verified that the waveguiding properties of a photonic quasicrystal structure with 8-fold rotational symmetry are affected by the presence of defect-free localized states within the photonic band gap.

The introduction of a perturbation (defect) in the linear channel alters the transmission through the waveguide. Actually, the defect affects the degeneracy of the resonant mode intrinsically localized in that position, allowing or preventing the signal propagation. This finding is analogous to what have been previously observed in numerical studies on add-and-drop filters based on both periodic [15] and quasiperiodic [16] dielectric structures. In those works two parallel linear waveguides are coupled by means of an extrinsic defect. Here we use instead a single waveguide and exploit the *intrinsic* defect of the quasiperiodic structure. In all these cases the presence of two degenerate modes with opposite symmetries seems to favour the propagation in the backward direction and to inhibit the propagation in the forward direction. Consequently the EM properties of the waveguide can be tuned changing the defect characteristics (radius, dielectric constant, position).

Obviously, since these peculiar effects are associated to the presence of a localized stated, their EM behaviour is extremely confined in terms of frequency, suggesting that 8-fold quasicrystalline structure can be exploited for the realisation of photonic tunable notch filters having very narrow bandwidth and a large attenuation.

#160960 - $15.00 USD Received 4 Jan 2012; revised 28 Feb 2012; accepted 5 Mar 2012; published 2 Nov 2012